Resonant high-order harmonic generation from plasma ablation: Laser intensity dependence of the harmonic intensity and phase

D. B. Milošević[1,2]
[1]*Faculty of Science, University of Sarajevo, Zmaja od Bosne 35, 71000 Sarajevo, Bosnia and Herzegovina*
[2]*Max-Born-Institut, Max-Born-Str. 2a, D-12489 Berlin, Germany*
(Received 12 October 2009; published 3 February 2010)

Experimentally observed strong enhancement of a single high-order harmonic in harmonic generation from low-ionized laser plasma ablation is explained as resonant harmonic generation. The resonant harmonic intensity increases regularly with the increase of the laser intensity, while the phase of the resonant harmonic is almost independent of the laser intensity. This is in sharp contrast with the usual plateau and cutoff harmonics, the intensity of which exhibits wild oscillations while its phase changes rapidly with the laser intensity. The temporal profile of a group of harmonics, which includes the resonant harmonic, has the form of a broad peak in each laser-field half cycle. These characteristics of resonant harmonics can have an important application in attoscience. We illustrate our results using examples of Sn and Sb plasmas.

DOI: 10.1103/PhysRevA.81.023802 PACS number(s): 42.65.Ky, 42.50.Hz, 32.80.Rm, 52.38.Mf

I. INTRODUCTION

The generation of high-order harmonics by irradiating atoms with an intense short laser pulse was observed more than 20 years ago (for reviews see Refs. [1–5]). In this process, due to the nonlinear interaction with the strong electric field of the laser pulse, the medium emits coherent radiation at frequencies that are multiples (up to a few hundred [6,7]) of the laser field frequency ω. The high-harmonic intensity is characterized by a long plateau in which all harmonics have almost the same intensity. For a linearly polarized laser pulse, this plateau consists of odd harmonics and finishes with an abrupt cutoff at the energy $3.173U_P + 1.325I_P$ [8]. Here $U_P = I/(4\omega^2)$ (in atomic units) is the electron ponderomotive energy, with I the laser intensity and $I_P = -E_1$ the ground-state ionization energy.

More recently, high-order harmonic generation (HHG) was discovered in experiments with preformed plasma plumes. It was shown that this medium (i.e., the ablated plasma) also generates high-order harmonics characterized by a plateau and a cutoff. The role of atoms is now taken by the plasma ions [9] (for recent reviews see Refs. [10,11]).

The main problem of HHG from atomic gases is its low conversion efficiency. It is up to a few times 10^{-5} for HHG by a linearly polarized laser field [12], while it can be slightly higher for HHG by two-color field combinations [13,14]. However, in experiments with laser plasma ablation strong resonance enhancement of single harmonics with conversion efficiency $\sim 10^{-4}$ was observed [15–21]. Another advantage of the ablation medium is a wider selection of the target material. The resonant enhancement was observed in In [15], Sn [16], GaAs [17,18], InSb [18], Cr [18], Sb [19], nanoparticles [20], and Te [21] plasmas. For more references see the recent reviews in Refs. [10,11]. The positive ions of the mentioned plumes have a large absorption strength for the transition between the ground state 1 and the excited state 2. This excited state is metastable and is embedded in the continuum so that the excitation energy $\Delta\omega = E_2 - E_1 > I_P$. The resonant enhancement was observed for the laser frequency ω such that $\Delta\omega = (2n_R + 1)\omega$, n_R integer. The conversion efficiency depends on the oscillator strength and it was the highest for In II [15].

For application of this ultrashort coherent extreme ultraviolet (XUV) sources it is not only necessary to generate intense high harmonics, but it is also very important to analyze characteristics of these harmonics (pulse duration, wavelength, coherence, focusability, divergence, etc.). Such an analysis was performed for HHG from atomic gases (see, for example, Ref. [2]), but for plasma harmonics a lot of effort in this direction still needs to be done [10,11]. The first reconstruction of the electromagnetic field of the harmonic spectrum generated from Cr plasma was presented at the conferences in Refs. [22,23]. Using the method of reconstruction of attosecond beating by interference of two-photon transitions (RABITT) [24], in [22,23] the attosecond pulse trains with 300 as duration were reconstructed. This result shows that the plasma harmonics are also sources of attosecond pulses, similar to gas harmonics. However, this experiment concerns regular plateau harmonics in Cr II. More precisely, five odd harmonics between the 11th and 19th were taken into account. The question is how the resonant harmonics (for Cr II this is the harmonic 29) behave in this context. This is important because the intensity of resonant harmonics is much higher, making them an excellent candidate for various applications [25–27].

In the present contribution we first introduce our model of resonant HHG in Sec. II. In the following two sections we analyze the dependence on the laser intensity of both the plateau and the resonant harmonics intensity and phase. In Sec. V we analyze the temporal profile of groups of harmonics, mode-locking of which enables attosecond pulse train generation. Finally, our conclusions are given in Sec. VI.

II. THEORETICAL MODEL OF RESONANT HIGH-ORDER HARMONIC GENERATION

We recently introduced a theoretical model of resonant HHG [28] (see also recent application of this model to more complex systems and comparison with the experiment [29]).

This model is based on the generalization of the Lewenstein *et al.* [8] model to HHG from a coherent superposition of states [30,31]. The model introduced in Ref. [28] assumes that the ground state having the energy $E_1 < 0$ and the excited state ($E_2 > 0$) have different parity so that it is possible to form a coherent superposition of these states in an excitation process (the excitation energy is $\Delta\omega = E_2 - E_1$ and the resonant enhancement was observed for the large absorption strength of the transition $1 \rightarrow 2$). In accordance with the three-step-model picture of HHG, in the resonant HHG the laser-driven electron wave packet starts from the excited state of the single charged plasma ablation ion and after propagation in the continuum, it finishes in the ground ionic state, which is resonantly coupled to this excited state. During the recombination to the ground state, a high harmonic having the energy Ω is emitted. In Fig. 1 we schematically present the previously described process of resonant HHG. In this process the parity has to be conserved. The ionic states have different parity, which gives the parity -1. One high-harmonic photon also contributes to the parity by -1. Therefore, the even number of photons $2k$ has to be exchanged with the laser field to conserve the parity $-1 = -1 \times (-1)^{\pm 2k}$. This gives the resonant high-harmonic energy $\Omega = \Delta\omega \pm 2k\omega, k = 0, 1, 2, \ldots,$. If the resonant condition $\Delta\omega = (2n_R + 1)\omega$ is fulfilled, we will have the emission of odd harmonics at the frequencies

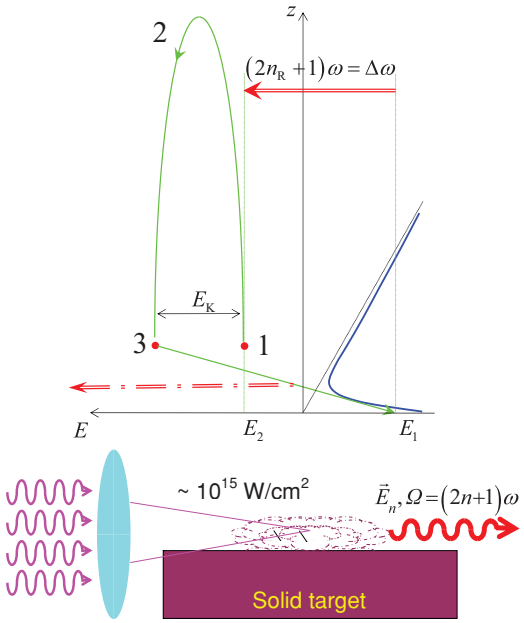

FIG. 1. (Color online) Laser ablation plasma is created by focusing a laser pulse, having duration of the order of 1 ps to 1 ns and the intensity of 10^{10} W/cm^2, on a solid target. A shorter (~30 fs) and stronger (~10^{15} W/cm^2) linearly polarized laser pulse is focused on this plasma and high harmonics of frequency $\Omega = (2n + 1)\omega$ are emitted. In the upper part of the figure the three-step model of resonant HHG is depicted. The states with energies E_1 and E_2 have different parity and the excited state is embedded in the continuum ($E_2 > 0$). In step 1 the electron is ionized from the excited state of the ion and then, in step 2, it propagates in the laser field acquiring the kinetic energy E_K. In step 3 the electron recombines to the ground state E_1 and a harmonic photon of frequency $\Omega = \Delta\omega \pm 2k\omega = [2(n_R \pm k) + 1]\omega$ is emitted.

$\Omega = (2n_R + 1)\omega, (2n_R + 1 \pm 2)\omega, \ldots,$. The standard single-state high harmonics having the energy $(2n + 1)\omega$ are also emitted.

The harmonic intensity is defined by $\Omega^4|D(\Omega)|^2$, where the harmonic strength is $D(\Omega) = |D(\Omega)| \exp[i\Phi(\Omega)] \approx a_1 a_2 D_{12}(\Omega)$, with a_1 and a_2 the initial amplitudes of the ionic bound states in the superposition of states 1 and 2 (for simplicity we choose $a_1 = a_2 = 1/\sqrt{2}$). $D_{12}(\Omega)$ is the Fourier transform of the time-dependent dipole.

It should also be mentioned that the previous results for resonant HHG were recently confirmed using a Floquet-based formalism [32]. The influence of the plasma characteristics on resonant HHG was studied in Ref. [33] and the results obtained are consistent with the model of Ref. [28]. Furthermore, very recently [34] it was shown that the influence of atomic autoionizing states on the phase matching of HHG may result in the efficient selection of the single harmonic, which explains why in the experiments only the enhancement of a single resonant harmonic was observed.

III. DEPENDENCE OF THE HARMONIC INTENSITY ON THE LASER INTENSITY

We first show numerical results for the Sn, keeping in mind that all other target materials for which the resonant enhancement of HHG was observed have qualitatively similar behavior. The Sn II ($I_P = 14.632$ eV) has the gf values 1.52 for the transitions $^2P_{3/2} \rightarrow (^1D)^2D_{5/2}$ for which $\Delta\omega = 26.27$ eV (see Table 1 in Ref. [35]). The laser wavelength that corresponds to the resonance of $\Delta\omega$ with the 17th harmonic is 802 nm. As our second example, we consider Sb II ($I_P = 16.63$ eV), which has the gf values 1.36 for the transitions $^3P^2 \rightarrow (^2D)^3D_3$ for which $\Delta\omega = 32.79$ eV (see Table 4 in Ref. [36]). The resonance of $\Delta\omega$ with the 21st harmonic appears for the wavelength 794 nm. We will first explore how the harmonic intensity changes with the laser intensity.

In Fig. 2 we present, in false colors, the harmonic intensity for Sn II as a function of the laser intensity, which changes from 2×10^{13} to 5.2×10^{14} W/cm^2, and the harmonic order. It is obvious that the harmonic 17 is strongly enhanced for all intensities. Other harmonics form a plateau with a cutoff in accordance with the $3.173U_P + 1.325I_P$ cutoff law, which forms a diagonal in Fig. 2. Analogous results for Sb II are presented in Fig. 3. In this case the harmonic 21 is strongly enhanced.

In our simulations we neglected the depletion of the initial states. Using the method of Ref. [37], generalized to the p ground state [38], we found that for a 30-fs laser pulse having the peak intensity 5.2×10^{14} W/cm^2 10% of ions survive the intensity 1.38×10^{14} W/cm^2 (1.93×10^{14} W/cm^2) for Sn II (Sb II) so that the depletion effect becomes important only for higher intensities. Furthermore, in Ref. [31] we explored the depletion effect for HHG from a coherent superposition of the $1s$ and $2s$ hydrogen-like states and found that it affects only the low-energy part of the spectrum, which corresponds to HHG from the excited state alone and which is not of interest in the present article. It should also be mentioned that our results are obtained using the single-active electron approximation (SAEA). This approximation provides a good description of

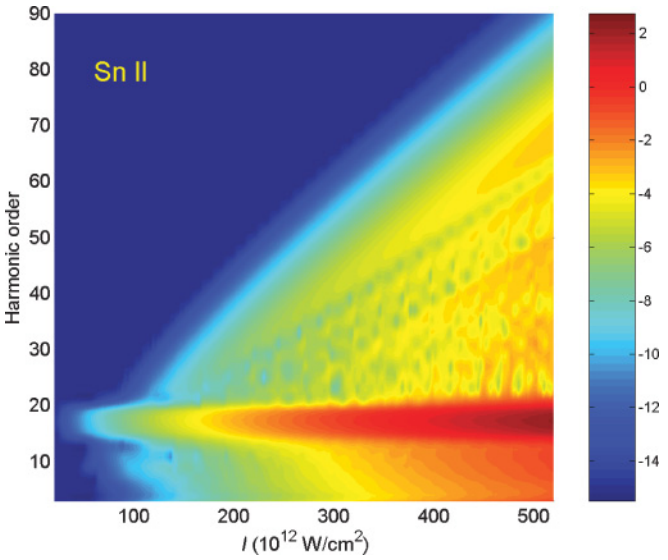

FIG. 2. (Color online) The harmonic intensity, presented in false colors, as a function of the laser intensity and harmonic order for HHG from Sn II. The laser wavelength is 802 nm and its intensity changes from 2×10^{13} to 5.2×10^{14} W/cm^2.

the ionization dynamics of the rare gases that have a closed shell. Analysis of the ionization of open-shell atoms is more complicated. Both the experiment [39] and theory [40] showed a dramatic suppression of ionization relative to the SAEA expectations. The conventional SAEA theory overestimates ionization by orders of magnitude. Since Sn II and Sb II have open shells we expect that these ions can survive higher intensity. In our model we also neglected the nonradiative decay of the excited state that is embedded in the continuum. Let us discuss this. For example, the linewidth of the relevant excited state of Sb II is 137 m eV [36]. This corresponds to the decay time of 4.804 fs = 1.814 optical cycles. Since the harmonic emission happens on the time scale of a small part of

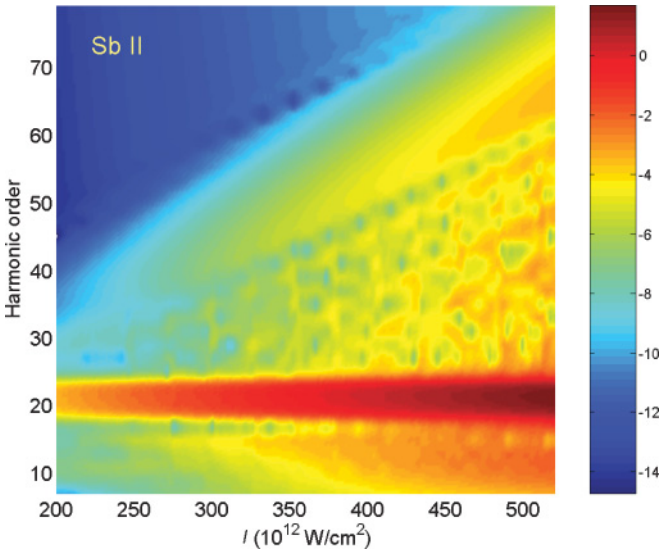

FIG. 3. (Color online) Same as in Fig. 2 but for HHG from Sb II, the wavelength 794 nm, and the intensity from 2×10^{14} to 5.2×10^{14} W/cm^2.

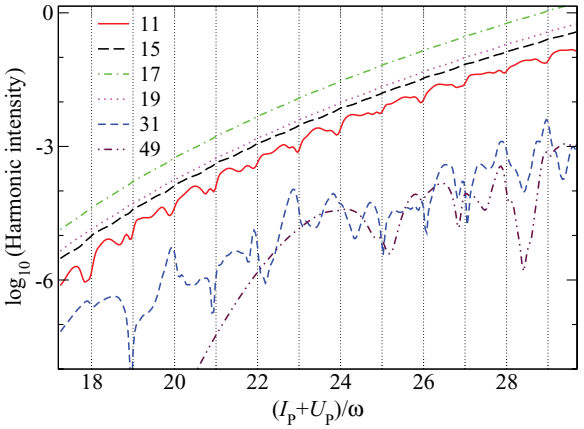

FIG. 4. (Color online) The intensities of the harmonic 11 (red solid line), 15 (black long dashed line), 17 (green dot-dashed line), 19 (magenta dotted line), 31 (blue dashed line), and 49 (maroon double-dot dashed line), as functions of the parameter $(I_P + U_P)/\omega$, for HHG from Sn II by a linearly polarized laser field having the wavelength 802 nm. The intensity of the harmonics 15, 17, and 19 is divided by 100.

the optical cycle it is not necessary to consider the nonradiative decay of the excited states.

Let us now analyze the dependence of particular harmonic intensities on the laser intensity in more detail. In Fig. 4 we show (for Sn II) the dependence of the intensities of the harmonics 11, 15, 17, 19, 31, and 49 on the laser intensity, expressed through the dimensionless parameter $n_c = (I_P + U_P)/\omega$, for the laser intensity from 2×10^{14} to 5.2×10^{14} W/cm^2 (notice that the intensity of the much stronger resonant harmonic is divided by 100). For the single-state HHG this parameter is important since the enhancements, the physical origin of which is different than that of the resonant harmonic, appear for integer values of n_c (this is related to the closings of the channel n_c [41]). The harmonic 11 is in the lower part of the plateau and below the resonant harmonic 17, while the harmonic 31 is in the middle of the plateau and above the resonance. The intensities of the harmonics 11 and 31 show an increasing oscillatory dependence on the laser intensity. In Ref. [41] this was explained as the interference of the contributions of many quantum orbits (see also Refs. [42–44] for details of the quantum-orbit theory). At the channel closings the harmonic intensity exhibits a threshold behavior, which manifests as a constructive interference of a large number of quantum-orbit contributions leading to two types of enhancements [45]. For the higher harmonic order 49 the harmonic intensity first grows rapidly (but without oscillations) with the increase of the laser intensity. This is the cutoff region in which only one quantum orbit contributes [42,43]. When the harmonic enters the plateau region the contributions of several quantum orbits began to interfere leading to the oscillatory structure shown in Fig. 4. Such behavior of the harmonic intensity is well known and was described in detail in Refs. [2,42,43]. We are interested here in the behavior of the resonant harmonic 17. From Fig. 4 we see that the increase of the 17th harmonic intensity with the laser intensity is quite regular. There are no traces of oscillations, which are characteristic for the single-state HHG.

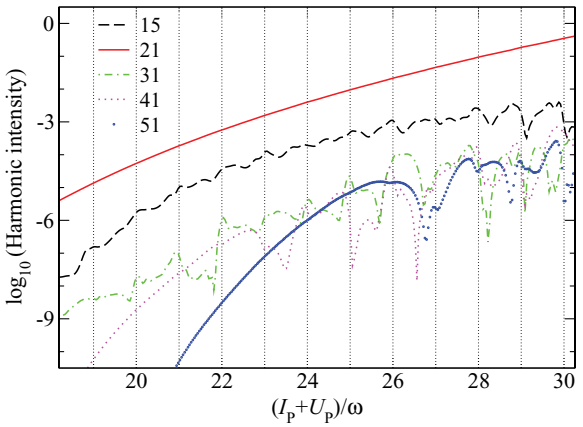

FIG. 5. (Color online) The intensities of the harmonic 15 (black dashed line), 21 (red solid line; the intensity is divided by 100), 31 (green dot-dashed line), 41 (magenta dotted line), and 51 (blue circles), as functions of the parameter $(I_P + U_P)/\omega$, for HHG from Sb II by a linearly polarized laser field having the wavelength 794 nm.

Such behavior is similar to that of low-order harmonics [31]. The harmonics 15 and 19 are neighbor harmonics to the resonant harmonic 17 and can be considered as low-order harmonics with respect to it, which explains their similar nonoscillatory behavior as a function of the laser intensity.

In Fig. 5 we show results analogous to that of Fig. 4, but for Sb II. In this case, the resonant harmonic is 21 so that we decided to show the dependence of the intensities of the harmonics 15, 21, 31, 41, and 51 on the parameter n_c, for the same laser intensity interval as in Fig. 3. The harmonic 15 (black dashed line) is in the lower part of the plateau and below the resonant harmonic 21 (red solid line), while the harmonic 31 (green dot-dashed line) is in the middle of the plateau and above the resonant harmonic. As expected, the intensities of the harmonics 15 and 31 show an increasing oscillatory dependence on the laser intensity. The harmonic intensities of the harmonics 41 (magenta dotted line) and 51 (blue circles) first grow rapidly (cutoff region) and then have a lot of oscillations (plateau region). The cutoff region is longer for the harmonic 51 so that the mentioned oscillations start for a higher intensity than for the harmonic 41. The increase of the resonant 21st harmonic intensity with the laser intensity is quite regular. Again, there are no oscillations that are characteristic for the single-state HHG.

IV. DEPENDENCE OF THE HARMONIC PHASE ON THE LASER INTENSITY

Let us now analyze the dependence of the harmonic phase on the laser intensity. It is known that for the single-state HHG the harmonic phase changes rapidly with the laser intensity (more precisely, it decreases linearly as $-U_P\tau$ where τ is the travel time of the corresponding quantum orbit [2,42,43]). The phases of the harmonics 49 and 51, presented in Figs. 6 (for Sn II) and 7 (for Sb II), respectively, really show such a behavior: They decrease linearly with the increase of the laser intensity [except for high intensities near channel closings for $n_c \geqslant 25$ (for Sn II) or $n_c \geqslant 27$ (for Sb II); for Sb II the exceptions are also low laser intensities for $n_c < 20$]. In the Sn II example, shown in Fig. 6, the 13th harmonic phase also decreases with the increase of the laser intensity, except in the regions near channel closings. This decrease is not so rapid as for the harmonic 49 phase. A similar conclusion is valid for the Sb II example and the harmonics 15 and 51 in Fig. 7.

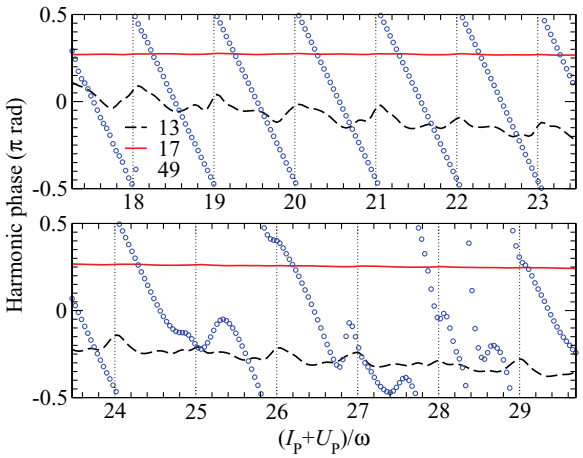

FIG. 6. (Color online) The phases of the harmonic 13 (black dashed line), 17 (red solid line), and 49 (blue circles), as functions of the parameter $(I_P + U_P)/\omega$, for HHG from Sn II. The laser wavelength is 802 nm.

The most impressive result shown in Fig. 6 is that the phase of the resonant harmonic 17 is almost constant. It changes from 0.757 to 0.868 rad. Let us estimate the phase of the harmonic $\Omega = \Delta\omega$. For short travel times ($\tau \approx 0$), from Eqs. (20) and (21) and the Appendix C in Ref. [31] it follows that

$$D(\Omega) \approx D_{12}(\Omega) \propto \int dt e^{i\Omega t} d_{12}(t) \propto i \int dt e^{i\Omega t} \times [\cos(\Delta\omega t) - \sin(\Delta\omega t)] f(t) \propto \delta_{\Omega,\Delta\omega} e^{i\frac{\pi}{4}}. \quad (1)$$

This approximate result $\Phi = \pi/4 = 0.7854$ rad is in excellent agreement with the previous numerical results. In the case of Sb II (Fig. 7) an analogous result for the phase of the resonant

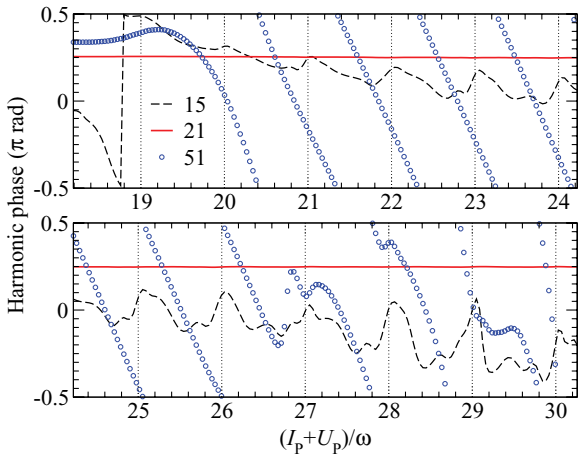

FIG. 7. (Color online) The phases of the harmonic 15 (black dashed line), 21 (red solid line), and 51 (blue circles), as functions of the parameter $(I_P + U_P)/\omega$, for HHG from Sb II. The laser wavelength is 794 nm.

harmonic 21 is that it changes from 0.772 to 0.805 rad, which is again in excellent agreement with the approximate result $\Phi = \pi/4$. As we will see in the next section, this unexpected behavior of the resonant harmonic phase can have important consequences for applications.

V. MODE-LOCKING OF HIGH HARMONICS AND THE ATTOSECOND PULSE TRAIN GENERATION

By mode-locking of several high harmonics it is possible to generate a train of attosecond pulses. This train can be quantitatively characterized by associating to each harmonic the field $E_n(t) = n^2 \exp(-in\omega t)D(n)$, where $D(n)$ is the previously defined nth harmonic strength. Combining a group of N subsequent harmonics, starting from a fixed harmonic n_0, we define the ratio R of the coherent over the incoherent sum of harmonic intensities [4,42,46,47]

$$R(n_0, N; t) = \left| \sum_{n=n_0}^{n_0+N-1} E_n(t) \right|^2 \Bigg/ \sum_{n=n_0}^{n_0+N-1} |E_n(t)|^2, \qquad (2)$$

where t is the harmonic emission time. If the amplitudes of all N modes of the harmonic field are equal, then the ratio (2) varies from $R = 1$ (for modes that are oscillating in a random fashion) to $R = N$ when all modes oscillate in phase.

In Fig. 8 we show the ratio (2) for different groups of odd harmonics for HHG from Sn II. The group of odd harmonics from 45 to 55 (blue dot-dashed line) shows a behavior typical for the single-state HHG: Two dominant peaks in each half cycle correspond to long and short orbits of the Lewenstein *et al.* model [8,42]. For HHG from Sb II a similar behavior has the group of odd harmonics from 41 to 51 (blue dot-dashed line in Fig. 9). The temporal profile of the group of odd harmonics from the 3rd to the 13th (harmonics below the resonance for Sn II in Fig. 8) and the group of odd harmonics from the harmonic 3 to 17 (for Sb II in Fig. 9) show a similar behavior: There is a structure that repeats in each half cycle (red dashed line). This structure is more complicated due to the contribution of more quantum orbits. On the other hand, the group of harmonics that includes the resonant harmonic 17 (for Sn II) or the harmonic 21 (for Sb II) shows a completely different behavior. There is one broad peak in the middle of the optical cycle. The shape of this peak does not depend on the number of harmonics included. In Fig. 8 the result for the interval 15–19 (black solid line) almost overlaps with the result for the longer interval 11–23 (cyan dotted line). The corresponding full width at half maximum is between 468 and 489 as. Analogous results for Sb II are shown in Fig. 9: The corresponding harmonic intervals are 19–23 and 15–27, while the full width at half maximum is from 462 to 482 as.

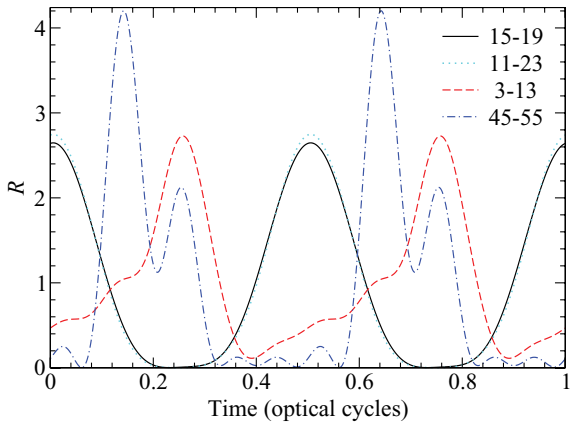

FIG. 8. (Color online) The ratio of the coherent over the incoherent sum of the harmonic intensities as a function of the time during one optical cycle. The results for the groups of odd harmonics, as indicated in the legend, are presented. HHG is from Sn II, the laser intensity is 4×10^{14} W/cm^2, and the laser wavelength is 802 nm.

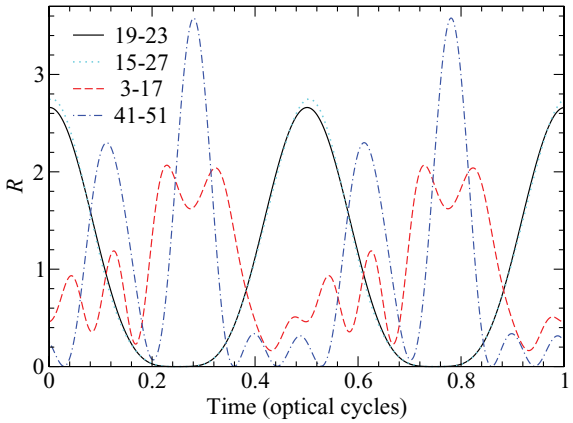

FIG. 9. (Color online) Same as in Fig. 8, but for HHG from Sb II, the laser intensity 4×10^{14} W/cm^2, and the wavelength 794 nm.

It is important to notice that for the atomic HHG by a linearly polarized laser field four attosecond pulses are generated during one optical cycle. It is possible, by appropriate focusing, to select two pulses from these four pulses per cycle since the collective effects due to the macroscopic propagation select the short or long trajectories of the Lewenstein model [2]. Recently, such an attosecond train of two pulses per cycle was obtained by phase locking of five harmonics generated from Cr plasma [22,23]. However, in the case of resonant harmonics the previously mentioned selection of pulses by appropriate focusing is not necessary since we already have only one peak in the laser-field half cycle. This can simplify the experimental setup. Furthermore, due to the larger time interval between the pulses in the train we expect that the resonant HHG by a few-cycle laser field is a good candidate for the isolated attosecond pulse generation [26,27].

VI. CONCLUSION

In conclusion, we find that the laser intensity dependence of the intensity and phase of the single harmonic generated in resonant HHG from plasma ablation is different than that of the standard plateau and cutoff high harmonics. The resonant harmonic intensity increases continuously (i.e., without rapid oscillations) with the increase of the laser intensity, while the resonant harmonic phase is almost constant. Such unusual (for HHG) behavior of the harmonic phase requires a detailed experimental investigation. Namely, the harmonic phase dependence is important for synchronization of high-order harmonics. The subfemtosecond light pulses can be obtained by superposing several high-order harmonics [24,25].

In the context of recent first attosecond pulse train reconstruction of high-order harmonics from laser ablation plasma [22,23] the results of the present work are even more important. We find that the temporal profile of a group of odd harmonics, which encompasses the resonant harmonic is in the form of a broad peak in each laser-field half cycle. This is an advantage in comparison with the usual plateau and cutoff harmonics where two such peaks are generated per half-cycle, which requires the appropriate experimental technique (i.e., such focusing that the collective effects due to the macroscopic propagation select only one peak). Taking into account a smooth dependence of the harmonic intensity on the laser intensity and that it is not necessary to manipulate with long and short orbits by appropriate focusing, we expect that the resonant HHG has a bright perspective for application in attoscience [26,27].

ACKNOWLEDGMENTS

We enjoyed discussions with R. A. Ganeev, L. B. Elouga Bom, T. Ozaki, P. Salières, and V. V. Strelkov. Support by the Federal Ministry of Education and Science, Bosnia and Herzegovina is gratefully acknowledged.

[1] V. T. Platonenko and V. V. Strelkov, Quantum Electron. **28**, 564 (1998).
[2] P. Salières, A. L'Huillier, Ph. Antoine, and M. Lewenstein, Adv. At. Mol. Opt. Phys. **41**, 83 (1999).
[3] W. Becker, F. Grasbon, R. Kopold, D. B. Milošević, G. G. Paulus, and H. Walther, Adv. At. Mol. Opt. Phys. **48**, 35 (2002).
[4] D. B. Milošević and F. Ehlotzky, Adv. At. Mol. Opt. Phys. **49**, 373 (2003).
[5] H. C. Kapteyn, M. M. Murnane, and I. P. Christov, Phys. Today **58**, 39 (2005).
[6] E. Seres, J. Seres, F. Krausz, and C. Spielmann, Phys. Rev. Lett. **92**, 163002 (2004); J. Seres, E. Seres, A. J. Verhoef, G. Tempea, C. Streli, P. Wobrauschek, V. Yakovlev, A. Scrinzi, C. Spielmann, and F. Krausz, Nature (London) **433**, 596 (2005).
[7] O. Cohen, X. Zhang, A. L. Lytle, T. Popmintchev, M. M. Murnane, and H. C. Kapteyn, Phys. Rev. Lett. **99**, 053902 (2007).
[8] M. Lewenstein, Ph. Balcou, M. Yu. Ivanov, A. L'Huillier, and P. B. Corkum, Phys. Rev. A **49**, 2117 (1994).
[9] R. Ganeev, M. Suzuki, M. Baba, and H. Kuroda, Opt. Lett. **30**, 768 (2005).
[10] R. A. Ganeev, J. Phys. B **40**, R213 (2007).
[11] R. A. Ganeev, Sov. Phys. Usp. **52**, 55 (2009).
[12] E. Constant, D. Garzella, P. Breger, E. Mével, Ch. Dorrer, C. Le Blanc, F. Salin, and P. Agostini, Phys. Rev. Lett. **82**, 1668 (1999).
[13] D. B. Milošević and W. Sandner, Opt. Lett. **25**, 1532 (2000).
[14] I. J. Kim, C. M. Kim, H. T. Kim, G. H. Lee, Y. S. Lee, J. Y. Park, D. J. Cho, and C. H. Nam, Phys. Rev. Lett. **94**, 243901 (2005); I. J. Kim, G. H. Lee, S. B. Park, Y. S. Lee, C. H. Nam, T. Mocek, and K. Jakubczak, Appl. Phys. Lett. **92**, 021125 (2008).
[15] R. A. Ganeev, M. Suzuki, M. Baba, H. Kuroda, and T. Ozaki, Opt. Lett. **31**, 1699 (2006); R. A. Ganeev, H. Singhal, P. A. Naik, V. Arora, U. Chakravarty, J. A. Chakera, R. A. Khan, I. A. Kulagin, P. V. Redkin, M. Raghuramaiah, and P. D. Gupta, Phys. Rev. A **74**, 063824 (2006).
[16] M. Suzuki, M. Baba, R. Ganeev, H. Kuroda, and T. Ozaki, Opt. Lett. **31**, 3306 (2006).
[17] R. A. Ganeev, H. Singhal, P. A. Naik, V. Arora, U. Chakravarty, J. A. Chakera, R. A. Khan, P. V. Redkin, M. Raghuramaiah, and P. D. Gupta, J. Opt. Soc. Am. B **23**, 2535 (2006).
[18] R. A. Ganeev, P. A. Naik, H. Singhal, J. A. Chakera, and P. D. Gupta, Opt. Lett. **32**, 65 (2007).
[19] M. Suzuki, M. Baba, H. Kuroda, R. A. Ganeev, and T. Ozaki, Opt. Express **15**, 1161 (2007).
[20] R. A. Ganeev, M. Suzuki, P. V. Redkin, M. Baba, and H. Kuroda, Phys. Rev. A **76**, 023832 (2007); R. A. Ganeev, Laser Physics **18**, 1009 (2008).
[21] M. Suzuki, M. Baba, H. Kuroda, R. A. Ganeev, and T. Ozaki, J. Opt. Soc. Am. B **24**, 2686 (2007).
[22] L. B. Elouga Bom, S. Haessler, P. Salières, and T. Ozaki, "The first attosecond pulse train reconstruction of high-order harmonics from laser ablation plasma", in *Conference on Lasers and Electro-Optics/Quantum Electronics and Laser Science Conference, San Jose, CA, 04–09 May 2008*, Vols 1–9, pp. 1361–1362.
[23] T. Ozaki, L. B. Elouga Bom, J. Abdul-Hadi, R. A. Ganeev, S. Haessler, and P. Salières, "High intensity high-order harmonics generated from low-density plasma", AIP Conf. Proc. – July 25, 2009 – Volume 1153, pp. 254–262, in *Laser-Driven Relativistic Plasmas Applied to Science, Industry and Medicine: 2nd International Symposium*, Kyoto (Japan), 19–23 January 2009.
[24] P. M. Paul, E. S. Toma, P. Breger, G. Mullot, F. Augé, Ph. Balcou, H. G. Muller, and P. Agostini, Science **292**, 1689 (2001).
[25] Y. Mairesse, A. de Bohan, L. J. Frasinski, H. Merdji, L. C. Dinu, P. Monchicourt, P. Breger, M. Kovačev, R. Taïeb, B. Carré, H. G. Muller, P. Agostini, and P. Salières, Science **302**, 1540 (2003).
[26] P. Agostini and L. F. DiMauro, Rep. Prog. Phys. **67**, 813 (2004); **67**, 1673 (2004).
[27] F. Krausz and M. Ivanov, Rev. Mod. Phys. **81**, 163 (2009).
[28] D. B. Milošević, J. Phys. B **40**, 3367 (2007).
[29] R. A. Ganeev and D. B. Milošević, J. Opt. Soc. Am. B **25**, 1127 (2008).
[30] J. B. Watson, A. Sanpera, X. Chen, and K. Burnett, Phys. Rev. A **53**, R1962 (1996); A. Sanpera, J. B. Watson, M. Lewenstein, and K. Burnett, *ibid.* **54**, 4320 (1996).
[31] D. B. Milošević, J. Opt. Soc. Am. B **23**, 308 (2006).
[32] I. A. Ivanov and A. S. Kheifets, Phys. Rev. A **78**, 053406 (2008).
[33] L. B. Elouga Bom, F. Bouzid, F. Vidal, J. C. Kieffer, and T. Ozaki, J. Phys. B **41**, 215401 (2008).
[34] I. A. Kulagin and T. Usmanov, Opt. Lett. **34**, 2616 (2009).
[35] G. Duffy, P. van Kampen, and P. Dunne, J. Phys. B **34**, 3171 (2001).
[36] R. D'Arcy, J. T. Costello, C. McGuinness, and G. O'Sullivan, J. Phys. B **32**, 4859 (1999).

[37] S. V. Popruzhenko, V. D. Mur, V. S. Popov, and D. Bauer, Phys. Rev. Lett. **101**, 193003 (2008); Laser Physics **108**, 947 (2009).
[38] D. B. Milošević, W. Becker, M. Okunishi, G. Prümper, K. Shimada, and K. Ueda, J. Phys. B **43**, 015401 (2010).
[39] M. Smits, C. A. de Lange, A. Stolow, and D. M. Rayner, Phys. Rev. Lett. **93**, 213003 (2004).
[40] Z. X. Zhao and T. Brabec, J. Phys. B **39**, L345 (2006).
[41] D. B. Milošević and W. Becker, Phys. Rev. A **66**, 063417 (2002).
[42] Ph. Antoine, M. Gaarde, P. Salières, B. Carré, A. L'Huillier, and M. Lewenstein, in *Multiphoton Processes 2006*, edited by P. Lambropoulos and H. Walther, Institute of Physics Conference Series Number 154 (Institute of Physics Publishing, Bristol, 1997), p. 142.
[43] P. Salières, B. Carré, L. Le Déroff, F. Grasbon, G. G. Paulus, H. Walther, R. Kopold, W. Becker, D. B. Milošević, A. Sanpera, and M. Lewenstein, Science **292**, 902 (2001).
[44] D. B. Milošević, D. Bauer, and W. Becker, J. Mod. Opt. **53**, 125 (2006).
[45] D. B. Milošević, E. Hasović, S. Odžak, and W. Becker, J. Mod. Opt. **55**, 2653 (2008).
[46] Ph. Antoine, A. L'Huillier, and M. Lewenstein, Phys. Rev. Lett. **77**, 1234 (1996).
[47] D. B. Milošević, W. Becker, R. Kopold, and W. Sandner, Laser Physics **11**, 165 (2001).